www.sciencemag.org/cgi/content/full/330/6012/1797/DC1

Supporting Online Material for

High-Flux Solar-Driven Thermochemical Dissociation of CO_2 and H_2O Using Nonstoichiometric Ceria

William C. Chueh, Christoph Falter, Mandy Abbott, Danien Scipio, Philipp Furler, Sossina M. Haile,* Aldo Steinfeld*

*To whom correspondence should be addressed. E-mail: smhaile@caltech.edu (S.M.H.); aldo.steinfeld@ethz.ch (A.S.)

Published 24 December 2010, *Science* **330**, 1797 (2010)
DOI: 10.1126/science.1197834

This PDF file includes:

High-Flux Solar-Driven Thermochemical Dissociation of CO_2 and H_2O using Nonstoichiometric Ceria

William C. Chueh, Christoph Falter, Mandy Abbott, Danien Scipio, Philipp Furler, Sossina M. Haile, Aldo Steinfeld

Supporting Online Materials

Materials

CeO_2 (Alfa Aesar 11328) was ball-milled with 16 wt% starch (Mallinckrodt 8188-2) for 19 to 24 h in anhydrous ethanol, and, after drying, mixed with 42 wt% graphite powders
(-100 mesh, Alfa Aesar 14735). The composite powder was uniaxially pressed into quarter-circular-arc pieces. Subsequent heat-treatment at 1,500° C for 5 hr induced both thermal decomposition of the starch and graphite poreformers and sintering to yield suitably mechanically robust porous monoliths. The pieces measured approximately 40 mm in arc length, 8 mm in thickness, 9 mm in height. Porosity was determined by a simple measurement of the geometric dimensions and sample mass and comparing to the theoretical density of CeO_2, 7.2 g cm^{-3}; it was found to be 80 %. X-ray powder diffraction data were collected using a Philip X'Pert PRO diffractometer (Cu kα, 45 kV, 40mA). Scanning electron microscopy was performed on a Carl-Zeiss 1550 VP.

Experimental Methods

The solar reactor is designed as a cavity-receiver that allows the efficient capture of incoming concentrated solar radiation, Fig. 1. It consists of a cylindrical volume 102 mm in both inner diameter and height, with a 4 cm-diameter circular aperture. Its apparent total absorptivity – as determined by Monte Carlo ray-tracing – exceeds 0.94 (*S1*). A highly-reflective compound parabolic concentrator (CPC) (*S2*) is incorporated at the aperture to augment the solar flux concentration and reduce re-radiation losses. The cavity is closed by a 3 mm-thick clear fused quartz window mounted in front of the CPC on a water-cooled copper ring that also serves as a shield for spilled radiation. The cavity walls are made from Inconel 600 and are lined with thermally-insulating porous alumina tiles 2.5 cm in thickness. Reacting gases were injected through four inlets into the annular gap between the porous ceria cylinder and the alumina insulation tiles. Product gases exited the cavity through an axial outlet port at the bottom. Experiments were conducted at Paul Scherrer Institute's High-Flux Solar Simulator (HFSS) (*S3*): an array of ten 15 kW_e high-pressure xenon arcs, each closed-coupled with truncated ellipsoidal specular reflectors of common focus. This unique facility provides an external source of intense thermal radiation, mostly in the visible and infrared spectra, that closely approximates the heat transfer characteristics of highly concentrating solar systems such as solar towers

and solar parabolic dishes. Power flux intensities were adjustable by the number of Xe arcs in operation, the position of the venetian-blind shutter, and the position of the solar reactor relative to the focal plane. Radiative fluxes incident into the solar reactor were measured optically with a calibrated CCD camera on a water-cooled Al_2O_3-plasma coated Lambertian target, positioned at the aperture plane. Incident radiative power was obtained by numerical integration of the measured fluxes and verified by a calorimeter. Gaseous products were analyzed on-line by gas chromatography (Agilent High Speed Micro G2890A, detection threshold: 10 ppm, sampling rate: ~0.01 Hz), supplemented by an infrared-based detector for CO and CO_2 (Siemens Ultramat-23, detection threshold: 0.2 %, sampling rate ~1 Hz), by a thermal conductivity-based detector for H_2 (Siemens Calomat 6, detection threshold: 50 ppm, sampling rate: ~1 Hz), and by a paramagnetic alternating pressure-based detector for O_2 (Siemens Oxymat 6, detection threshold: 50 ppm, sampling rate: ~1 Hz). A micropump on each device was used to sample a small fraction of the effluent gas from the reactor. Gas compositions were converted to flow rates by using Ar as an internal reference. Uncertainty in flow rates was estimated by propagating the accuracy of the Ar mass flow controller and the accuracy of the measured gas composition (per manufacturer specification). The total pressure, given the open flow system, was approximately 1 atm for all experiments, with the balance being Ar.

To examine oxygen and fuel evolution under differential reaction conditions, 0.429 g of ceria was loaded into a horizontal alumina tube reactor (9.5 mm in inner diameter) that is placed inside an infrared furnace (Ulvac-Riko VHT-E44). A thermocouple, enclosed in alumina sheath, was placed in direct contact with the sample. Digital mass flow controllers delivered dry and humidified Ar (via a water bubbler) as well as dry CO_2. The effluent gas composition was analyzed using a Pfeiffer Thermostar GSD301 quadrupole mass spectrometer, calibrated using six known amounts of O_2, H_2, and CO.

Efficiency Calculation

In theory, solar energy input is necessary only during the endothermic oxygen-evolution reaction during which the metal oxide is thermally reduced. We define the instantaneous solar-to-fuel energy conversion efficiency as:

$$\eta = \frac{r_{fuel}\Delta H_{fuel}}{P_{solar} + r_{inert}E_{inert}}$$

where r_{fuel} is the molar fuel production rate (taken to be the rate of oxygen evolution multiplied by a stoichiometric factor), ΔH_{fuel} is the higher heating value (HHV) of the fuel, P_{solar} is the incident solar radiation power, r_{inert} is the flow rate of the inert gas during oxygen evolution, and E_{inert} is the energy required to separate the nitrogen sweep gas from air (in this work, Ar was utilized as the sweep gas purely for reasons of experimental convenience). We take E_{inert} to be 20 kJ mol^{-1} *(S4)*. The instantaneous efficiency does not explicitly include the amount of

the fuel produced nor power input necessary to maintain reaction temperature during the exothermic step. Neglecting these contributions does not significant impact the calculated efficiency in the performed solar experiments because the rate of fuel evolution is orders of magnitude greater than the rate of oxygen evolution.

The average solar-to-fuel energy conversion efficiency is given as:

$$\eta = \frac{\Delta H_{fuel} \int r_{fuel} dt}{\int P_{solar} dt + E_{inert} \int r_{inert} dt}$$

This definition takes into account the amount of fuel evolved as well as solar energy input during that step. Comparisons to literature values are made only for systems in which the efficiency calculation has been carried out in a similar fashion (total fuel energy out to total solar and parasitic energy in). In some reports, efficiencies are calculated using the lower heating value (LHV) of the fuel produced. To facilitate direct conversion, it is noted that for H_2, LHV = 0.85 × HHV, whereas for CO, LHV = HHV.

Reactor Energy Balance

For simplicity, the chemical reaction is assumed to proceed to completion and temperature gradients are neglected. Assuming a blackbody cavity-receiver, the re-radiation power through the aperture is:

$$P_{reradiation} = P_{solar} \frac{\sigma T^4}{IC}$$

where P_{solar} is the incident solar power, σ is the Stefan-Boltzmann constant, T is the nominal cavity-receiver temperature, I is the direct normal irradiance (DNI, taken to be 1 kW m^{-2}), and C is the solar concentration ratio. The heat loss due to heating the inert gas (Ar) is:

$$P_{inert} = r_{inert} c_p \Delta T$$

where r_{inert} is the inert gas (molar) flow rate, c_p is the heat capacity under constant pressure, and ΔT is temperature difference of the gas at the inlet and in the reactor. The remainder of the power loss, namely $P_{solar} - r_{fuel} \Delta H_{fuel} - P_{reradiation} - P_{inert}$, is due to a combination of conductive, radiative, and convective losses at the reactor wall, some of which is due to active water-cooling.

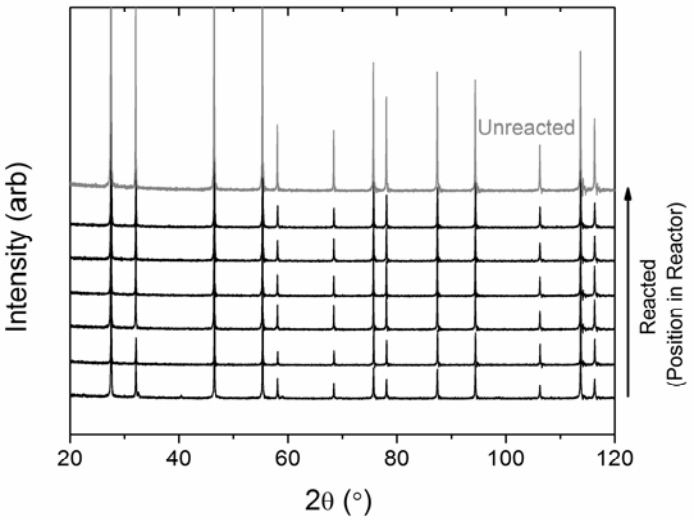

Fig. S1: X-ray diffraction patterns collected from an as-prepared (unreacted) ceria monolith (upper trace) and those used in the thermochemical process (reacted, lower traces) showing the absence of significant reaction between the porous ceria monolith and the reactor wall materials.

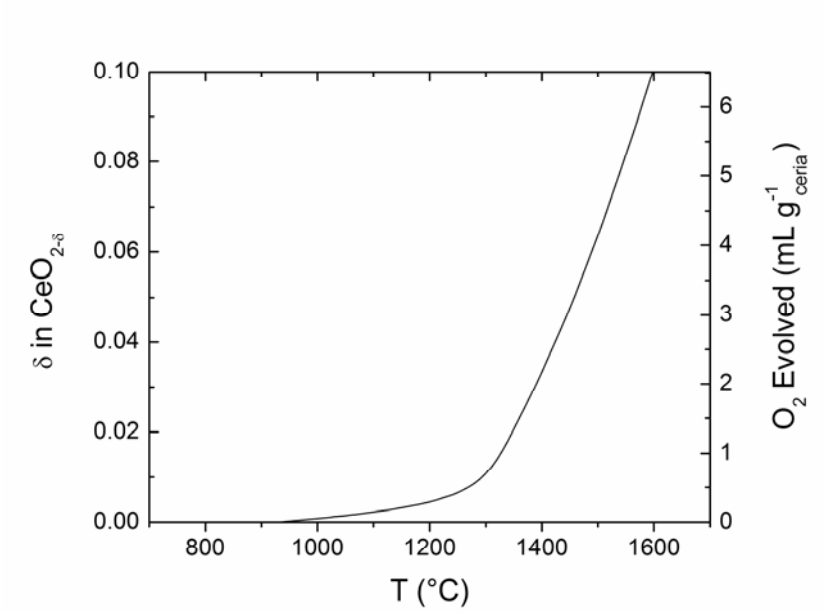

Figure S2: Equilibrium oxygen nonstoichiometry (δ) in $CeO_{2-\delta}$ at $pO_2 = 10^{-5}$ atm as measured by thermogravimetry. Data above 1500 °C were extrapolated using measured enthalpy and entropy values. After Panlener *et al*. (*S5*)

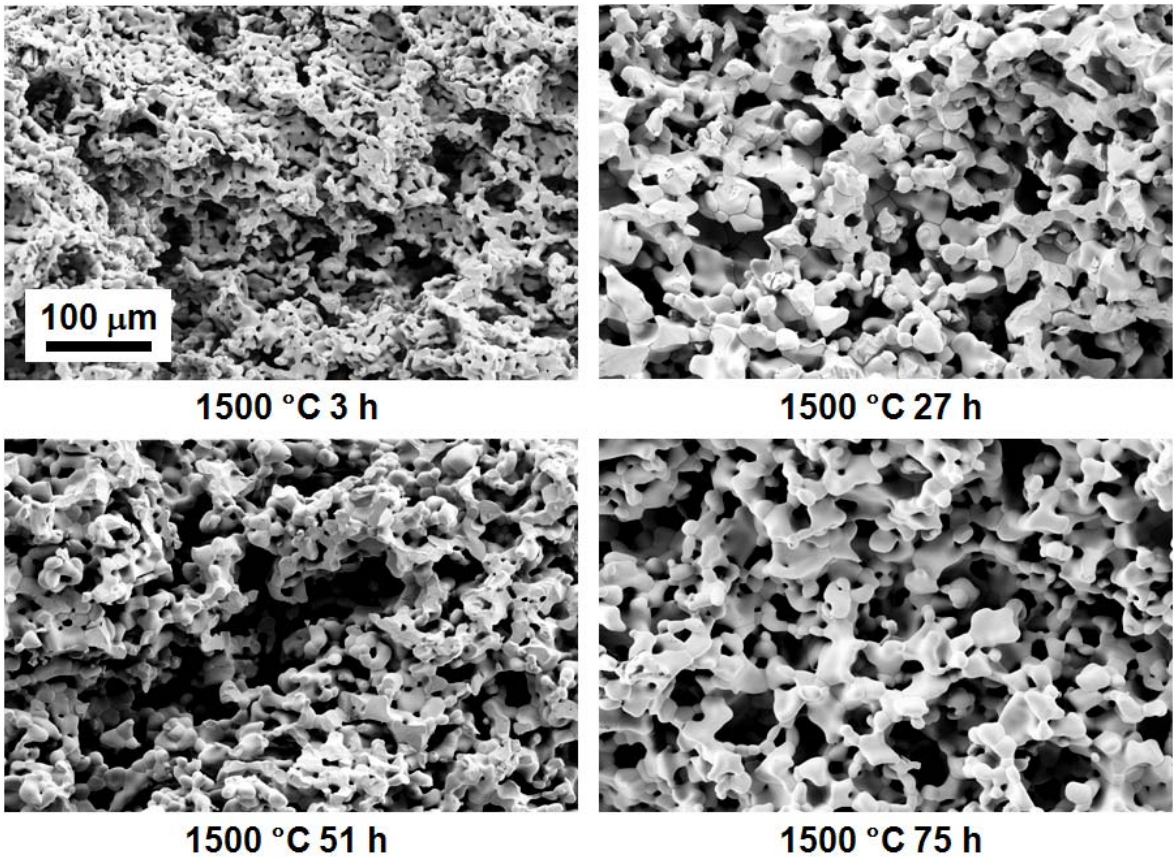

Figure S3: Evolution in the ceria morphology after heat-treatment of the materials at 1,500 °C for the indicated number of hours. Scale is the same for all four images.

References

S1. S. Kraeupl, A. Steinfeld, Monte Carlo radiative transfer modeling of a solar chemical reactor for the co-production of zinc and syngas. *J. Sol. Energy-T. ASME* **127**, 102 (2005).

S2. W. T. Welford, R. Winston, *High Collection Nonimaging Optics*. (Academic Press, San Diego, 1989).

S3. J. Petrasch *et al.*, A 50-kW 11,000-suns novel high-flux solar simulator based on an array of Xenon arc lamps. *J. Sol. Energy Eng.* **129**, 405 (2007).

S4. H.-W. Haring, *Industrial Gases Processing*. (Wiley-VCH, 2008).

S5. R. J. Panlener, R. N. Blumenthal, J. E. Garnier, A Thermodynamic Study of Nonstoichiometric Cerium Dioxide. *J. Phys. Chem. Solids* **36**, 1213 (1975).